arXiv:1402.0893v1 [cond-mat.str-el] 4 Feb 2014

$CaIrO_3$: a Spin-Orbit Mott Insulator Beyond the $j_{\rm eff} = 1/2$ Ground State

M. Moretti Sala,[1,*] K. Ohgushi,[2] A. Al-Zein,[1] Y. Hirata,[2] G. Monaco,[3,1] and M. Krisch[1]

[1] *European Synchrotron Radiation Facility, BP 220, F-38043 Grenoble Cedex, France*
[2] *Institute for Solid State Physics, University of Tokyo, Kashiwa, Chiba 277-8581, Japan*
[3] *Dipartimento di Fisica, Università di Trento, via Sommarive 14, 38123 Povo (TN), Italy*

In $CaIrO_3$ electronic correlation, spin-orbit coupling, and tetragonal crystal field splitting are predicted to be of comparable strength. However, the nature of its ground state is still object of debate, with contradictory experimental and theoretical results. We probe the ground state of $CaIrO_3$ and assess the effective tetragonal crystal field splitting and spin-orbit coupling at play in this system by means of resonant inelastic x-ray scattering. We conclude that insulating $CaIrO_3$ is *not* a $j_{\rm eff} = 1/2$ iridate and discuss the consequences of our finding to the interpretation of previous experiments. In particular, we clarify how the Mott insulating state in iridates can be readily extended beyond the $j_{\rm eff} = 1/2$ ground state.

Spin-orbit coupling is the main ingredient for $5d$ transition metal oxides to form novel electronic states of matter, such as the recently discovered Mott insulating state in Sr_2IrO_4 [1–3]. This insulating behaviour is unexpected in iridates perovskites as, for a half-filled shell with spatially extended orbitals, electronic correlation was thought to be negligible. Instead, the role of electronic correlation is enhanced here by spin-orbit coupling, through the formation of the so-called $j_{\rm eff} = 1/2$ ground state. Its realization arises from the interaction of strong spin-orbit coupling ($\zeta \sim 0.5$ eV) and cubic crystal field (10Dq ~ 3 eV), and is perturbed by short- and long-ranged anisotropies which could cause departures from the $j_{\rm eff} = 1/2$ ground state [4–7]. A small, but sizable tetragonal contribution $|\Delta| \sim 0.01$ eV to the cubic crystal field 10Dq was detected in both Sr_2IrO_4 [6] and Ba_2IrO_4 [7], with opposite signs, in agreement with recent theoretical calculations [5]. In these cases, however, $|\Delta| \ll \zeta \ll$ 10Dq and the $j_{\rm eff} = 1/2$ ground state in Sr_2IrO_4 and Ba_2IrO_4 is not in doubt. Structural distortions are instead more pronounced in the insulating post-perovskite $CaIrO_3$ [8]; thus the cubic symmetry of the crystal field is expected to be drastically lowered and the $j_{\rm eff} = 1/2$ ground state to be severely altered. The robustness of the $j_{\rm eff} = 1/2$ ground state against structural distortions, in particular octahedral rotations and elongations, as well as chemical substitution has been mostly tested by means of resonant X-ray magnetic scattering (RMXS), on the basis of the nearly vanishing intensity at the L_2 absorption edge [3]. Following this criterion, a number of "$j_{\rm eff} = 1/2$ iridates" have been identified [9–13], including $CaIrO_3$ [14]. However, this interpretation has been widely controversed [15–17]. Indeed, a unified picture has not been reached yet: the interpretation of RMXS results [14], was supported by LDA+SO+U [18], but contradicted by *ab-initio* quantum chemistry [19] calculations. The latter predict a large splitting of the t_{2g} states that give rise to a strongly unbalanced occupation of the xy, yz and zx orbitals, while for the $j_{\rm eff} = 1/2$ ground state the three orbitals contribute with an equal weight of 1/3. Remarkably, despite contradicting evidences about the details of the electronic ground state, consensus is reached on the magnetic interactions, with a strong antiferromagnetic coupling along the c-axis and a weak ferromagnetic one along the a-axis, which stabilize canted long range antiferromagnetism [20] and characterize $CaIrO_3$ as a quasi-one-dimensional antiferromagnet [19].

In this Letter, we use resonant inelastic X-ray scattering (RIXS) at the Ir L_3 edge to solve the puzzle of the ground state in $CaIrO_3$. RIXS is a powerful technique for the study of correlated electron systems mostly devoted to the study of high-T_c superconducting and insulating cuprates in the past years [21]. Recently, RIXS was applied to the investigation of magnetic excitations in correlated iridium oxides. Following the initial theoretical suggestion of Ament *et al.* [22], it was demonstrated that magnon dispersion could be studied in Sr_2IrO_4 [23, 24] and $Sr_3Ir_2O_7$ [25]. In the present work, we focus on the inelastic response of $CaIrO_3$ in the energy range relevant to spin-orbital excitations [23, 26–28] and we determine the effective tetragonal crystal field and spin-orbit coupling acting on t_{2g} levels by comparing the results to a single-ion model [17, 22, 27]. We obtain $\zeta = 0.52$ and $\Delta = -0.71$ eV and therefore conclude that the departure of $CaIrO_3$ from the $j_{\rm eff} = 1/2$ state is unambigous, in agreement with *ab-initio* calculations [19].

RIXS measurements were performed at the new inelastic X-ray scattering beamline of ESRF (ID20-UPBL06). Two different set-ups were used in order to optimize the flux and energy-resolution of the beamline. The incident radiation was monochromatized by a high heat-load double crystal Si(111) monochromator and a post-monochromator for further bandwidth reduction. In the high energy-resolution mode, a Si(844) back-scattering channel-cut reduced the incident photon bandwidth down to 15 meV at 11.215 keV [29]; in the low energy-resolution set-up, a Si(311) channel-cut monochromator provided a bandwidth of about 350 meV. A Kirkpatrick-Baez mirror system focused the X-rays to a spot size of 10×20 (V×H) μm^2 at the sample position. The scattered X-rays were energy-analyzed by a Rowland-type

spectrometer, equipped with 5 diced Si(844) analyzers (R = 2 m), and detected by a 5-element Maxipix detector, with a pixel size of 55×55 μm^2 [30]. The overall energy-resolution was about 25 (350) meV in the high (low) energy-resolution mode. A single crystal of $CaIrO_3$ was grown by the flux method as in Ref. 14. $CaIrO_3$ has a post-perovskite structure (space group $Cmcm$ [31]), composed of edge-sharing (corner-sharing) IrO_6 octahedra along the a-axis (c-axis), in which each octahedron is compressed along the corner-sharing O direction (the local z direction) with a bond length ratio of 0.97. Because of the alternating rotation of the octahedra around the a-axis, the local z- and the crystallographic c-axis form an angle of ±23°, thus forming a zig-zag chain of Ir-O-Ir bonds. The lattice parameters are a = 3.147, b = 9.859 and c = 7.290 Å [8]. $CaIrO_3$ is an insulator and undergoes a transition to a canted antiferromagnet at T_N = 115 K [20], in which the strong spin-orbit coupling stabilizes a striped-type magnetic order (magnetic moments are aligned parallely along a and mostly antiparallely along c, with a small canting in the direction of the b-axis) [14]. Throughout the experiment, the sample was kept at a temperature of 15 K.

Fig. 1 shows a low energy-resolution RIXS map of $CaIrO_3$. In RIXS, the incident photon energy is tuned to an absorption edge, the L_3 in our case, corresponding to the transition of an electron from the $2p_{3/2}$ to the 5d states, thus creating a deep core hole. The system then relaxes to a less excited final state by filling the core hole with the same or another electron, possibly creating a low energy excitation. The incident energy is scanned across the L_3 absorption line and spectra are recorded up to 12 eV energy loss. An elastic line and magnetic excitations are found close to the zero energy loss line. At increasing energy losses, we assign features to intra-t_{2g} ($t_{2g}^5 \rightarrow t_{2g}^5$), t_{2g}-to-e_g ($t_{2g}^5 \rightarrow t_{2g}^4 e_g^1$) and charge-transfer (CT) excitations (as indicated in the figure), following previous RIXS studies [32]. In this work, we concentrate on intra-t_{2g} excitations only. Their intensity (including that of the elastic line and magnetic excitations) is enhanced for incident photon energies about 3 eV below the main absorption peak. This is a common feature of several iridium oxides, which was observed in both RMXS and RIXS experiments [9, 26]. It can be understood by considering the electronic structure of an Ir^{4+} ion in a large cubic crystal field: with 5 electrons filling the 5d states, e_g states are empty and one hole is left in the t_{2g} states. The maximum of the absorption line (11.219 keV) corresponds to the transition of an electron into the 5d e_g state, while the contribution of the t_{2g} states is minor, as it scales with the number of unoccupied final states. On the other hand, it is reasonable to assume that intra-t_{2g} excitations are more effectively probed when a $2p_{3/2}$ electron is directly promoted in the 5d t_{2g} state, i.e. for incident photon energies tuned at ∼ 10Dq below the main absorption line (11.216 keV).

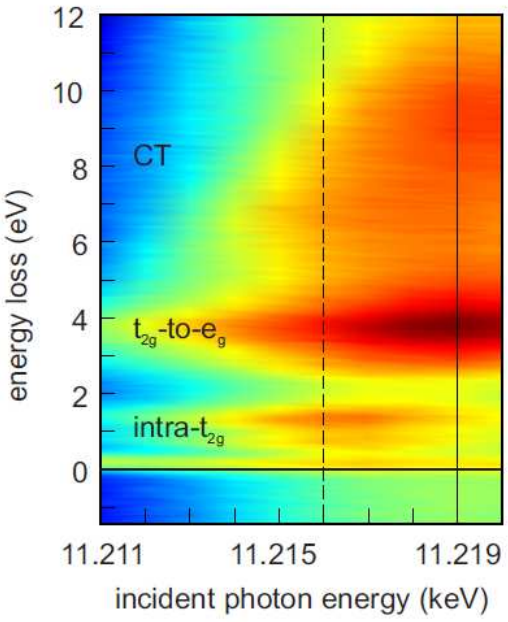

FIG. 1. RIXS color map of $CaIrO_3$. The continuous vertical line corresponds to the maximum of the absorption profile at 11.219 keV. The dashed vertical line, instead, corresponds to the incident photon energy used for the high energy-resolution RIXS spectrum of Fig. 2 (11.216 keV).

For the high resolution measurements, we fixed the incident photon energy at 11.216 keV to enhance t_{2g} excitations. A representative spectrum is shown in Fig. 2. The low energy range comprises the elastic line and a broad structure of magnetic origin, not discussed here. The 0.3-1.6 eV energy range is dominated by two intense broad features (B and C) and a weak, energy-resolution limited peak (A), similar to the excitation spectrum of Na_2IrO_3 and Li_2IrO_3 [28, 33]. The assignment of features B and C to local excitations across crystal field split states [28] was initially debated [34], but then supported by recent calculations [35]. We therefore assign features B and C of Fig. 2 in analogy to the case of Na_2IrO_3 and Li_2IrO_3. The assignment of features B and C is further strengthened by *ab-initio* calculations for $CaIrO_3$ predicting a splitting of the $j_{\rm eff}$ = 3/2 states by 0.6-0.7 eV [19], in agreement with the energy difference of about 0.6 eV for features B and C found in our experiment.

In the following we discuss the spin-orbit excitations (features B and C in Fig. 2) in more detail. Although of mostly local origin, it should be mentioned that they show a weak, but non negligible dispersion versus momentum transfer, in the order of 0.05 eV, indicating that they retain some non-local character. In the present work, however, we aim at determining the size of the effective tetragonal crystal field splitting and spin-orbit coupling in $CaIrO_3$ and the fine details of the band struc-

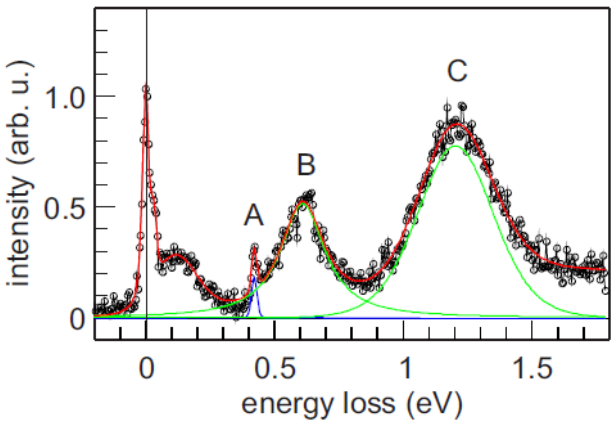

FIG. 2. RIXS spectrum of $CaIrO_3$ at a selected momentum transfer, $\mathbf{Q} = (1, 2, 10)$ r.l.u.. Continuous lines are fit to the experimental data.

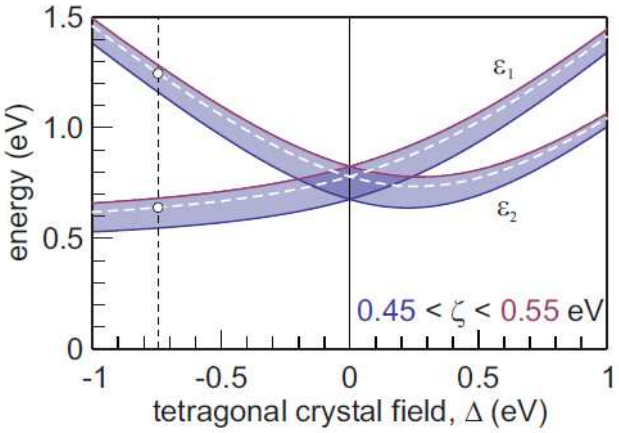

FIG. 3. Energy diagram of spin-orbit excitations calculated according to Eqs. (2) and (3) as a function of Δ for $0.45 < \zeta < 0.55$ eV. White dashed lines correspond to the estimated value of $\zeta = 0.52$ eV, while the white dots correspond to the actual value of the spin-orbit excitations in $CaIrO_3$.

ture will be neglected. In fact, their bandwidth is one order of magnitude smaller than the energy at which these excitations occur, and therefore inter-site interactions can be considered as small perturbations to the local crystal field. The *effective* parameters Δ and ζ then include any kind of renormalization due to non-local effects. A dedicated study of the transferred momentum dependence of such excitations is, however, desirable.

The spectra were fitted to three Pearson functions: feature A turns out to be energy-resolution limited, at an energy of about 0.42 eV, very similar to the value reported for Na_2IrO_3 and Li_2IrO_3 [28]. Features B and C are centered at 0.66 and 1.22 eV, respectively, which corresponds to the largest intra-t_{2g} splitting ever reported in iridium oxides. In order to better understand the nature of these excitations, and to assess the effective tetragonal crystal field splitting and spin-orbit coupling in $CaIrO_3$, we adopt a single-ion model [7, 14, 17, 22, 26, 27]. The weak momentum transfer dependence of these excitations suggests a dominant intra-site character, for which a local model is justified. Since 10Dq is sufficiently large (10Dq $\sim$ 3 eV), $5d$ e_g states are neglected and the interacting Hamiltonian for one *hole* in the $5d$ t_{2g} states is then written as

$$\mathcal{H} = \zeta \mathbf{L} \cdot \mathbf{S} - \Delta L_z^2, \qquad (1)$$

in which tetragonal crystal field splitting ($\Delta < 0$ for compressed octahedra) and spin-orbit coupling are treated on equal footing. For $\Delta = 0$, the ground state is represented by the $|j_{\rm eff} = 1/2\rangle$ doublet and the excited states by the $|j_{\rm eff} = 3/2\rangle$ quadruplet. For arbitrary values of ζ and Δ, the eigenstates of $\mathcal{H}$ are three non-degenerate Kramers doublets, which we generically label $|0, \pm\rangle$, $|1, \pm\rangle$ and $|2, \pm\rangle$ ($|0, \pm\rangle$ being the ground state wave function). The corresponding eigenvalues, E_0, E_1 and E_2, are reported, for example, in Ref. 17. Here we are interested in transitions from the $|0, \pm\rangle$ ground state to the $|1, \pm\rangle$ and $|2, \pm\rangle$ excited states. The corresponding energies, relative to the ground state, at which the RIXS transitions occur, are given by

$$\varepsilon_1 = E_1 - E_0 = \frac{\zeta}{4}\left[3 + \delta + \sqrt{9 + \delta(\delta - 2)}\right] \qquad (2)$$

$$\varepsilon_2 = E_2 - E_0 = \frac{\zeta}{2}\sqrt{9 + \delta(\delta - 2)}, \qquad (3)$$

where $\delta = 2\Delta/\zeta$. These are reported in Fig. 3 as a function of Δ for $0.45 < \zeta < 0.55$ eV. For $\Delta = 0$, $\varepsilon_1 = \varepsilon_2 = 3\zeta/2$ as the $|1, \pm\rangle$ and $|2, \pm\rangle$ states merge into the $|j_{\rm eff} = 3/2\rangle$ quadruplet when the $j_{\rm eff} = 1/2$ ground state is realized. In general, however, the energy of the two RIXS excitations is a function of both Δ and ζ.

In our case, the only solution with physical meaning is found by imposing $\varepsilon_1 = 0.66$ and $\varepsilon_2 = 1.22$ eV (white dots in the diagram of Fig. 3), from which one obtains $\zeta = 0.52$ and $\Delta = -0.71$ eV. The value of ζ compares favourably with previous estimates in other iridium oxides [7, 12, 26, 28], and in particular to the recently calculated value of 0.47 eV by Bogdanov *et al.* [19] for the specific case of $CaIrO_3$. The sign of Δ is consistent with structural studies reporting a compression of the IrO_6 octahedra [8], while its magnitude implies a minor contribution of the xy orbital to the ground state wave funtion (only 10%), in agreement with *ab-initio* quantum chemistry calculations which predict a splitting of t_{2g} states in the absence of spin-orbit coupling in the order of 0.63-0.76 [19]. Noteworthy, $|\Delta|$ is more than one order of magnitude larger than that of the prototypical $j_{\rm eff} = 1/2$ compounds, Sr_2IrO_4 ($\Delta = -0.01$ eV) [6] and Ba_2IrO_4 ($\Delta = 0.05$ eV) [17]. Therefore, $|\Delta| > \zeta$ and we

can safely state that $CaIrO_3$ is *not* a $j_{\rm eff} = 1/2$ iridate, with a dominant $(|yz, \mp\rangle \pm \imath|zx, \mp\rangle)/\sqrt{2}$ character of the ground state wave-function.

We now discuss the size and direction of the magnetic moments in comparison to existing experimental results and the sign of magnetic interactions. The size of the magnetic moment is a function of both ζ and Δ [17]: with the above determined values, the expectation value for the z component of the magnetic moment turns out to be 1.7 μ_B in $CaIrO_3$, i.e. larger than the magnetic moment of 1 μ_B expected for a perfectly localized $j_{\rm eff} = 1/2$ state. Following the interpretation of magnetization data of Ref. 14, we conclude that the magnetic moments in $CaIrO_3$ are canted along the b-axis, with a canting angle of $\sim 2°$, i.e. about 21° away from the local z-axis of the IrO_6 octahedra. It should be noted here that the discrepancy between RMXS and RIXS results is reconciled in view of their non-trivial dependence on magnetic moment direction [17]. Indeed, considering the actual value of Δ and ζ, and the direction of the magnetic moments, one obtains a Ir L_2/L_3 RMXS intensity ratio of 0.1%, which is below the detectability limit of 0.3% reported in the experiment [14] (the calculated Ir L_2/L_3 RMXS intensity ratio would be 24% in the case of magnetic moments aligned along the local z-axis). Magnetic interactions giving rise to the stripe-type canted antiferromagnetism of $CaIrO_3$ discussed above were explained in the framework of an ideal $j_{\rm eff} = 1/2$ state [14], for which theoretical arguments [36] predict antiferromagnetic (ferromagnetic) coupling along the corner-shared (edge-shared) bonds. $CaIrO_3$ seems to obey these rules. However, as long as the occupancy of the yz and zx orbitals is identical and their phase relation preserved, the same theoretical arguments apply and the sign of the magnetic interactions remains unchanged. Indeed, the fact that the coupling is ferromagnetic along a and antiferromagnetic along b, despite the severe departure of $CaIrO_3$ from the $j_{\rm eff} = 1/2$ ground state, is also supported by quantum chemistry calculations [19].

We are now in the position to discuss the transport properties of iridates and their connection to the $j_{\rm eff} = 1/2$ ground state. The latter was originally invoked to explain the insulating behaviour of Sr_2IrO_4 and readily extended to other "$j_{\rm eff} = 1/2$" compounds. In Fig. 4 we explain and extend the concept of a spin-orbit Mott insulator beyond the specific case of "$j_{\rm eff} = 1/2$" iridates. One has to consider the $5d$ t_{2g} states, whose bandwidth in the absence of perturbations would be too large for a reasonable Hubbard energy U to open a gap; rather, the density of states at the Fermi energy would be only slightly reduced, as in Fig. 4(b). Crucially, spin-orbit coupling in the absence of a tetragonal crystal field splits the otherwise degenerate t_{2g} states and a half filled $j_{\rm eff} = 1/2$ bands is isolated, with a much reduced bandwidth (w) compared to the original one. As $U > w$, lower (LHB) and upper (UHB) Hubbard bands are created,

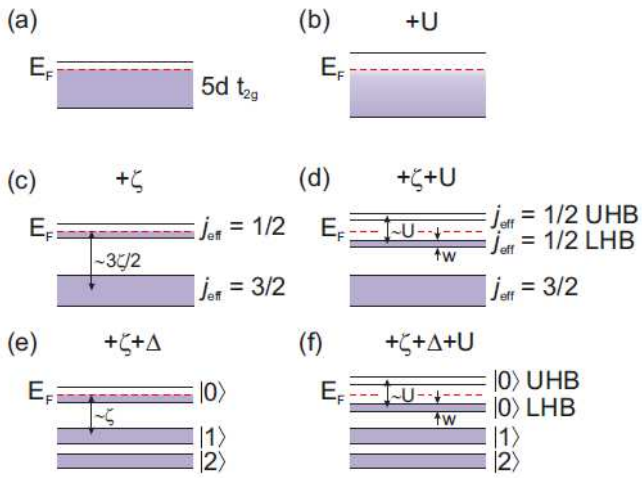

FIG. 4. Schematic representations of the band structure in iridates with $5d^5$ configurations in the absence of perturbations (a), with spin-orbit coupling (c) and spin-orbit coupling plus tetragonal crystal field splitting (e). Panels (b), (d) and (f) correspond to panels (a), (c) and (e), respectively, when the Hubbard term U is taken into account.

thus turning the system into an insulator (Fig. 4(d)) [1]. In the case of $CaIrO_3$, however, the large tetragonal crystal field degrades the $|j_{\rm eff} = 1/2\rangle$ ground state into the generic $|0\rangle$. Nevertheless, the smallest splitting between the $j_{\rm eff} = 1/2$- and $j_{\rm eff} = 3/2$-derived bands is ζ (ε_1 in the limit $\Delta \to -\infty$), i.e. only a factor 3/2 smaller than that in the pure $j_{\rm eff} = 1/2$ ground state. Therefore, for $U > w$ LHB and UHB bands are formed and the system retains its insulating character, although the ground state wave function differs significantly from $|j_{\rm eff} = 1/2\rangle$ (indeed, $|0, \pm\rangle = \pm|xy, \pm\rangle$ for $\Delta \to +\infty$ and $|0, \pm\rangle = (|yz, \mp\rangle \pm \imath|zx, \mp\rangle)/\sqrt{2}$ for $\Delta \to -\infty$). A rough estimate of U in $CaIrO_3$ can be naively extracted by adopting the interpretation, though debated [34, 35], of feature A in Fig. 2 as the excitation across the Mott gap [28]: we obtain $U \simeq 0.4$ eV which is consistent with the band gap of 0.34 eV deduced from resistivity measurements [18, 20] and places $CaIrO_3$ in the scenario of Fig. 4(f).

In conclusion, i) we solve the controversy concerning the ground state of $CaIrO_3$ [14, 19]: $CaIrO_3$ is *not* a $j_{\rm eff} = 1/2$ iridate, due to the large tetragonal crystal field. Indeed, we estimate the effective tetragonal crystal field splitting and spin-orbit coupling to be $\Delta = -0.71$ and $\zeta = 0.52$ eV, respectively, by inspecting the Ir L_3 edge RIXS response in the energy range relevant to spin-orbital excitations. ii) We show that experimental [14] and theoretical [19] results can be reconciled in view of the nontrivial dependence of the Ir L_2/L_3 RMXS intensity ratio on the magnetic moment direction [17]. Furthermore, iii) we understand that the sign of magnetic interactions is unchanged with respect to the ideal

$j_{\rm eff} = 1/2$ case because the even occupancy and the phase relation of the yx and zx orbitals is preserved. Finally, iv) we clarified how the Mott insulating state survives in $CaIrO_3$ despite the severe departure from the $j_{\rm eff} = 1/2$ ground state.

Acknowledgments - Enlightening discussions with G. Jackeli are kindly acknowledged. The experiment largely profited from technical support and expertise of R. Verbeni and C. Henriquet.

* marco.moretti@esrf.fr

[1] B. J. Kim, H. Jin, S. J. Moon, J. Kim, B. Park, C. S. Leem, J. Yu, T. W. Noh, C. Kim, S. Oh, J. Park, V. Durairaj, G. Cao, and E. Rotenberg, Physical Review Letters **101**, 076402 (2008).

[2] S. J. Moon, H. Jin, K. W. Kim, W. S. Choi, Y. S. Lee, J. Yu, G. Cao, A. Sumi, H. Funakubo, C. Bernhard, and T. W. Noh, Physical Review Letters **101**, 226402 (2008).

[3] B. J. Kim, H. Ohsumi, T. Komesu, S. Sakai, T. Morita, H. Takagi, and T. Arima, Science **323**, 1329 (2009).

[4] V. M. Katukuri, H. Stoll, J. van den Brink, and L. Hozoi, Phys. Rev. B **85**, 220402 (2012).

[5] H. Zhang, K. Haule, and D. Vanderbilt, Phys. Rev. Lett. **111**, 246402 (2013).

[6] S. Boseggia, H. C. Walker, J. Vale, R. Springell, Z. Feng, R. S. Perry, M. Moretti Sala, H. M. Rønnow, S. P. Collins, and D. F. McMorrow, Journal of Physics: Condensed Matter **25**, 422202 (2013).

[7] M. Moretti Sala, M. Rossi, S. Boseggia, J. Akimitsu, N. B. Brookes, M. Isobe, M. Minola, H. Okabe, H. M. Ronnow, L. Simonelli, D. F. McMorrow, and G. Monaco, ArXiv e-prints (2013), arXiv:1312.0857 [cond-mat.str-el].

[8] S. Hirai, M. Welch, F. Aguado, and S. Redfern, Z. Kristallogr. **224**, 345 (2009).

[9] S. Boseggia, R. Springell, H. C. Walker, A. T. Boothroyd, D. Prabhakaran, D. Wermeille, L. Bouchenoire, S. P. Collins, and D. F. McMorrow, Phys. Rev. B **85**, 184432 (2012).

[10] S. Boseggia, R. Springell, H. C. Walker, A. T. Boothroyd, D. Prabhakaran, S. P. Collins, and D. F. McMorrow, Journal of Physics: Condensed Matter **24**, 312202 (2012).

[11] J. W. Kim, Y. Choi, J. Kim, J. F. Mitchell, G. Jackeli, M. Daghofer, J. van den Brink, G. Khaliullin, and B. J. Kim, Phys. Rev. Lett. **109**, 037204 (2012).

[12] S. Boseggia, R. Springell, H. C. Walker, H. M. Rønnow, C. Rüegg, H. Okabe, M. Isobe, R. S. Perry, S. P. Collins, and D. F. McMorrow, Phys. Rev. Lett. **110**, 117207 (2013).

[13] S. Calder, G.-X. Cao, S. Okamoto, J. W. Kim, V. R. Cooper, Z. Gai, B. C. Sales, M. D. Lumsden, D. Mandrus, and A. D. Christianson, ArXiv e-prints (2013), arXiv:1309.5411 [cond-mat.str-el].

[14] K. Ohgushi, J.-i. Yamaura, H. Ohsumi, K. Sugimoto, S. Takeshita, A. Tokuda, H. Takagi, M. Takata, and T.-h. Arima, Phys. Rev. Lett. **110**, 217212 (2013).

[15] L. C. Chapon and S. W. Lovesey, Journal of Physics: Condensed Matter **23**, 252201 (2011).

[16] D. Haskel, G. Fabbris, M. Zhernenkov, P. P. Kong, C. Q. Jin, G. Cao, and M. van Veenendaal, Phys. Rev. Lett. **109**, 027204 (2012).

[17] M. Moretti Sala, S. Boseggia, D. F. McMorrow, and G. Monaco, Phys. Rev. Lett. **112**, 026403 (2014).

[18] A. Subedi, Phys. Rev. B **85**, 020408 (2012).

[19] N. A. Bogdanov, V. M. Katukuri, H. Stoll, J. van den Brink, and L. Hozoi, Phys. Rev. B **85**, 235147 (2012).

[20] K. Ohgushi, H. Gotou, T. Yagi, Y. Kiuchi, F. Sakai, and Y. Ueda, Phys. Rev. B **74**, 241104 (2006).

[21] L. J. P. Ament, M. van Veenendaal, T. P. Devereaux, J. P. Hill, and J. van den Brink, Reviews of Modern Physics **83**, 705 (2011).

[22] L. J. P. Ament, G. Khaliullin, and J. van den Brink, Physical Review B **84**, 020403 (2011).

[23] J. Kim, D. Casa, M. H. Upton, T. Gog, Y.-J. Kim, J. F. Mitchell, M. van Veenendaal, M. Daghofer, J. van den Brink, G. Khaliullin, and B. J. Kim, Phys. Rev. Lett. **108**, 177003 (2012).

[24] A. Lupascu, J. P. Clancy, H. Gretarsson, Z. Nie, J. Nichols, J. Terzic, G. Cao, S. S. A. Seo, Z. Islam, M. H. Upton, J. Kim, A. H. Said, D. Casa, T. Gog, V. M. Katukuri, L. Hozoi, J. van den Brink, H. Stoll, and Y.-J. Kim, ArXiv e-prints (2013), arXiv:1312.4005 [cond-mat.str-el].

[25] J. Kim, A. H. Said, D. Casa, M. H. Upton, T. Gog, M. Daghofer, G. Jackeli, J. van den Brink, G. Khaliullin, and B. J. Kim, Phys. Rev. Lett. **109**, 157402 (2012).

[26] X. Liu, V. M. Katukuri, L. Hozoi, W.-G. Yin, M. P. M. Dean, M. H. Upton, J. Kim, D. Casa, A. Said, T. Gog, T. F. Qi, G. Cao, A. M. Tsvelik, J. van den Brink, and J. P. Hill, Phys. Rev. Lett. **109**, 157401 (2012).

[27] L. Hozoi, H. Gretarsson, J. P. Clancy, B.-G. Jeon, B. Lee, K. H. Kim, V. Yushankhai, P. Fulde, Y.-J. Kim, and J. van den Brink, ArXiv e-prints (2012), arXiv:1212.4009 [cond-mat.str-el].

[28] H. Gretarsson, J. P. Clancy, X. Liu, J. P. Hill, E. Bozin, Y. Singh, S. Manni, P. Gegenwart, J. Kim, A. H. Said, D. Cas a, T. Gog, M. H. Upton, H.-S. Kim, J. Yu, V. M. Katukuri, L. Hozoi, J. van den Brink, and Y.-J. Kim, Phys. Rev. Lett. **110**, 076402 (2013).

[29] M. Moretti Sala, C. Henriquet, L. Simonelli, R. Verbeni, and G. Monaco, Journal of Electron Spectroscopy and Related Phenomena **188**, 150

[30] C. Ponchut, J. M. Rigal, J. Clment, E. Papillon, A. Homs, and S. Petitdemange, Journal of Instrumentation **6**, C01069 (2011).

[31] M. Sugahara, A. Yoshiasa, A. Yoneda, T. Hashimoto, S. Sakai, M. Okube, A. Nakatsuka, and O. Ohtaka, American Mineralogist **93**, 1148 (2008).

[32] K. Ishii, I. Jarrige, M. Yoshida, K. Ikeuchi, J. Mizuki, K. Ohashi, T. Takayama, J. Matsuno, and H. Takagi, Physical Review B **83**, 115121 (2011).

[33] H. Gretarsson, J. P. Clancy, Y. Singh, P. Gegenwart, J. P. Hill, J. Kim, M. H. Upton, A. H. Said, D. Casa, T. Gog, and Y.-J. Kim, Phys. Rev. B **87**, 220407 (2013).

[34] K. Foyevtsova, H. O. Jeschke, I. I. Mazin, D. I. Khomskii, and R. Valentí, Phys. Rev. B **88**, 035107 (2013).

[35] B. H. Kim, G. Khaliullin, and B. I. Min, ArXiv e-prints (2013), arXiv:1307.0614 [cond-mat.str-el].

[36] G. Jackeli and G. Khaliullin, Phys. Rev. Lett. **102**, 017205 (2009).